Supporting Information

Synthesis of 5,10,15-triazaporphyrins – effect of benzo-annulation on the electronic structures

Soji Shimizu,* Yuki Ito, Kazuaki Oniwa, Shoma Hirokawa, Yoshiaki Miura, Osamu Matsushita, and Nagao Kobayashi*

Department of Chemistry, Graduate School of Science, Tohoku University, Sendai 980-8578, Japan

Contents:

i. Experimental

General procedure: Electronic absorption spectra were recorded on a JASCO V-570 spectrophotometer. Magnetic circular dichroism (MCD) spectra were recorded on a JASCO J-725 spectrodichrometer equipped with a JASCO electromagnet, which produces magnetic fields of up to 1.09 T (1 T = 1 tesla) with both parallel and antiparallel fields. The magnitudes were expressed in terms of molar ellipticity per tesla ($[\theta]_M$ / deg dm^3 mol^{-1} cm^{-1} T^{-1}). Fluorescence spectra were measured on a Hitachi F-4500 spectrofluorimeter. ^{1}H NMR spectra were recorded on a JEOL ECA-600 spectrometer (operating at 594.17 MHz) and a Bruker AVANCE 400 spectrometer (operating at 400.33 MHz) using a residual solvents as internal references for ^{1}H (δ = 7.26 ppm for $CDCl_3$ and 2.09 ppm for toluene-d_8). High resolution mass spectra were recorded on a Bruker Daltonics Apex-III spectrometer or on an AB SCIEX 4800 *Plus* MALDI TOF/TOF Analyzer. Preparative separations were performed by alumina gel column chromatography (Wako), preparative thin layer plate (Silica gel 60, F_{254}, Merck), and recycling preparative GPC-HPLC (JAI LC-9201 with preparative JAIGEL-2H, 2.5H, and 3H columns). All reagents and solvents were of commercial reagent grade and were used without further purification except where noted.

Crystallographic data collection and structure refinement: Suitable crystals of **1** and ruthenium complex of **3a** were obtained from slow evaporation of dichloromethane in the presence of water and slow diffusion of hexane into a chloroform solution in the presence of a slight amount of pyridine, respectively. Data collection for **1** and ruthenium complex of **3a** was carried out at at –173 °C on a Bruker APEXII CCD diffractometer with MoKα radiation (λ = 0.71073 Å). The structures were solved by direct methods (SHLEXS-97[1] or Sir 2004[2]) and refined using a full-matrix least square technique (SHELXL-97).[1] Yadokari-XG[3] software was used as a GUI for SHELXL-97. CCDC-862131 and 864016 contain the supplementary crystallographic data for **1** and ruthenium complex of **3a**, respectively. These data can be obtained free of charge from the Cambridge Crystallographic Data Centre via

www.ccdc.cam.ac.uk/data_request/cif.

There is one residual electron density larger than 1 in the unit cell of **1** probably due to the effect of electron-rich bromine atoms. Because of the presence of C_2 symmetry axis, the position of NH-hydrogen atom could not be determined and refined positionally restrained conditions using DFIX command. There are three DFIX restraints in the final refinement.

Some large Q peaks were found due to disorder of solvent molecule(s) in the case of ruthenium complex of **3a**, which is (are) mostly chloroform. As we failed to model them properly, the rest molecules were refined without the effect of the solvent molecule(s) by the Platon squeeze technique. Despite using Platon squeeze for smoothing, two residual Q peaks having electron densities greater than 1.0 (1.29) are still observed close to the central ruthenium mainly due to its large electron density. The *tert*-butyl substituents were also disordered. Therefore the substituent parts were refined under thermally and positionally restrained conditions, using DFIX, SIMU, ISOR, and DELU commands. There are 292 restraints in the final refinement, of which 16 for DFIX, 36 for DELU, 108 for SIMU, and 132 for ISOR commands.

Computational methods: The Gaussian 09[4] software package was used to carry out DFT and TDDFT calculations at the B3LYP/6-31G(d) level. Structural optimization was performed on model compounds of **3a**, **3b**, and **3c** in which the peripheral *tert*-butylphenyl substituents were replaced by hydrogen atoms or phenyl groups for simplicity.

General synthetic procedures:

5-Pentafluorophenyl-1,9-dibromodipyrromethene 1: To a dry THF solution (30 mL) of 5-pentafluorophenyldipyrromethane (0.50 g, 1.6 mmol) at –78 °C was added dropwise a THF solution (15 mL) of *N*-bromosuccinimide (0.63 g, 3.5 mmol). After the consumption of the starting material, 50 mL of aqueous $Na_2S_2O_3$ was added to the reaction mixture. The organic phase was extracted with dichloromethane, and the resultant mixture was dried over $MgSO_4$. A brown oil was obtained after removing solvent under reduced pressure. The oil was dissolved in THF (30 mL) and DDQ (0.50 g, 2.2 mmol) was added. The mixture was stirred for 10 min at r.t., and then passed through an alumina column. The target compound was purified by silica gel column chromatography, and **1** was obtained as a red powder (0.58 g, 1.2 mmol, 77%). MALDI-TOF-MS (m/z): 468.9 (calcd for $C_{15}H_6N_2F_5Br_2$ = 468.8 [M^++H]); ^{1}H NMR ($CDCl_3$, 400 MHz, 298 K): δ = 6.37 ppm (s, 4H; β-pyrrole); UV/vis ($CHCl_3$): λ_{max} [nm] = 456.

***meso*-Pentafluorophenyl-substituted dibenzo-5,10,15-triazaporphyrin 3a:** A mixture of **1** (0.12 g, 0.26 mmol) and 5,6-di-*p*-*tert*-butylphenyl-1,3-diiminoisoindoline **2a** (0.22 g, 0.54 mmol) in *p*-xylene (1.0 mL) was stirred at r.t. for a few seconds. After addition of dimethylaminoethanol (DMAE, 1.0 mL), the mixture was heated at 145 °C for 1 hour. The reaction mixture was purified by silica gel column chromatography using CH_2Cl_2/hexane (1:2 (v/v)), and the final purification was carried out by silica gel thin layer chromatography to provide **3a** as a blue powder (42 mg, 15%). HR-ESI-FT-ICR-MS (m/z): 1108.5052 (calcd for $C_{71}H_{63}N_7F_5$ = 1108.5060 [M^++H]); ^{1}H NMR ($CDCl_3$, 400 MHz, 298 K): δ = 9.14 (s, 2H; α-benzo), 8.98 (s, 2H; α-benzo), 8.43 (d, J = 4.40 Hz, 2H; β-pyrrole), 8.22 (d, J = 4.00 Hz, 2H; β-pyrrole), 7.52–7.42 (m,

16H; phenyl), 1.42 ppm (s, 36H; *t*-butyl); UV/vis ($CHCl_3$): λ_{max} [nm] (ε) = 376 (81200), 595 (61600), 633 (76400).

***meso*-Pentafluorophenyl-substituted dinaphtho-5,10,15-triazaporphyrin 3b: 3b** was synthesized from a reaction of **1** (0.15 g, 0.32 mmol) and 6,7-di-*p*-*tert*-butylphenyl-1,3-diiminobenz[f]isoindole **2b** (0.30 g, 0.65 mmol) in *p*-xylene (1.0 mL) and DMAE (1.0 mL) and similarly purified as in the case of **3a**. **3b** was then obtained as a green powder in 1.6% yield (6.0 mg). HR-ESI-FT-ICR-MS (*m*/*z*): 1208.5374 (calcd for $C_{79}H_{67}N_7F_5$ = 1208.5373 [M^++H]); ^{1}H NMR (toluene-d_8, 600 MHz, 298 K): δ = 9.19 (s, 2H; naphtho), 9.15 (s, 2H; naphtho), 8.28 (d, *J* = 4.20 Hz, 2H; β-pyrrole), 8.22 (s, 2H; naphtho), 8.21 (s, 2H; naphtho), 7.80 (d, *J* = 3.60 Hz, 2H; β-pyrrole), 7.50 (d, *J* = 8.40 Hz, 4H; phenyl), 7.45 (d, *J* = 7.80 Hz, 4H; phenyl), 7.33 (d, *J* = 8.40 Hz, 4H; phenyl), 7.30 (d, *J* = 7.80 Hz, 4H; phenyl), 1.31 (s, 18H; *t*-butyl), 1.29 ppm (s, 18H; *t*-butyl); UV/vis ($CHCl_3$): λ_{max} [nm] (ε) = 345 (130000), 601 (69400), 635 (104000), 655 (119000).

***meso*-Pentafluorophenyl-substituted 5,10,15-triazaporphyrin 3c: 3c** was synthesized from a reaction of **1** (1.7 g, 3.6 mmol) and 3,4-di-*p*-*tert*-butylphenyl-2,5-pyrrolinediimine **3c** (2.5 g, 6.9 mmol) in *p*-xylene (6.0 mL) and DMAE (6.0 mL) and similarly purified as in the case of **3a**. **3c** was then obtained as a purple powder in 0.11% yield (4.0 mg). HR-ESI-FT-ICR-MS (*m*/*z*): 1008.4745 (calcd for $C_{63}H_{59}N_7F_5$ = 1008.4747 [M^++H]); ^{1}H NMR ($CDCl_3$, 600 MHz, 298 K): δ = 9.16 (d, *J* = 4.80 Hz, 2H; β-pyrrole), 8.74 (d, *J* = 4.80 Hz, 2H; β-pyrrole), 8.33 (d, *J* = 7.80 Hz, 4H; phenyl), 8.28 (d, *J* = 8.40 Hz, 4H; phenyl), 7.72 (d, *J* = 6.60 Hz, 4H; phenyl), 7.61 (d, *J* = 8.40 Hz, 4H; phenyl), 1.53 (s, 18H; *t*-butyl), 1.52 (s, 18H; *t*-butyl), –1.29 ppm (s, 2H; inner-NH); UV/vis ($CHCl_3$): λ_{max} [nm] (ε) = 367 (62700), 564 (29300), 637 (43700).

Ruthenium complex of 3a: By following the literature procedure,[5] **3a** was reacted with triruthenium dodecacarbonyl in benzonitrile at 200 °C for an hour. Highly polar blue fraction in silica gel column was collected. The axial ligans at this statge were carbonyl, which was replaced by a pyridyl group during crystallization. MALDI-TOF-MS (*m*/*z*): 1207.3892 (calcd for $C_{71}N_7H_{60}F_5Ru$ = 1207.3874 [M^+–2CO]); UV/vis ($CHCl_3$): λ_{max} [nm] = 370, 594.

ii. X-ray crystal structure of 1

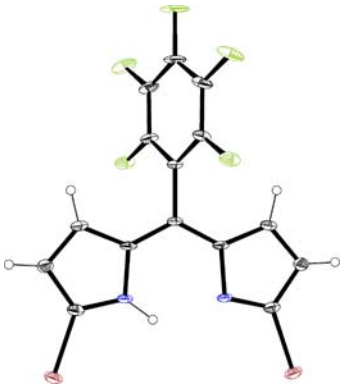

Figure S1. X-ray crystal structure of **1**. The thermal ellipsoids were scaled to the 50% probability level.

Crystallographic data for **1**: $C_{15}H_5N_2Br_2F_5$, M_w = 468.03, monoclinic, space group *C*2/c (no. 13), *a* = 13.432(6), *b* = 15.534(7), *c* = 7.285(3) Å, β = 93.759(6)°, *V* = 1516.6(12) Å^3, *Z* = 4, ρ_{calcd} = 2.050 g/cm^3, *T* = –173(2) °C, 5116 measured reflections, 1332 unique reflections (R_{int} = 0.0508), *R* = 0.0455 ($I > 2\sigma(I)$), R_w = 0.1309 (all data), GOF = 1.056, CCDC 862131.

iii. ^{1}H NMR spectra of 3a, 3b, and 3c

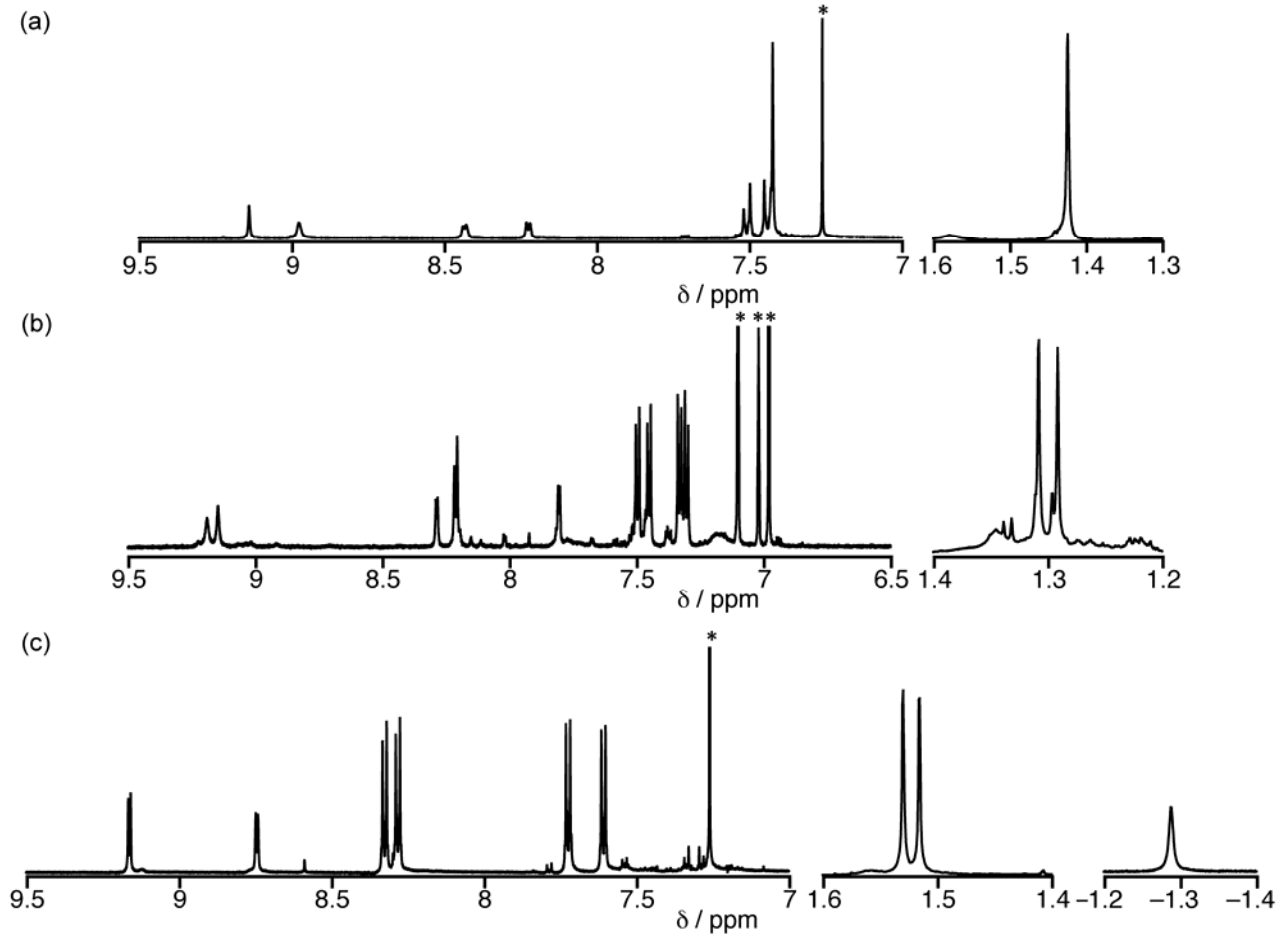

Figure S2. ^{1}H NMR spectra of **3a** (top), **3b** (middle), and **3c** (bottom) in $CDCl_3$ for **3a** and **3c** and in toluene-d_8 for **3b**. * indicates residual solvent peaks.

iv. Absorption and fluorescence spectra of 3a and 3b

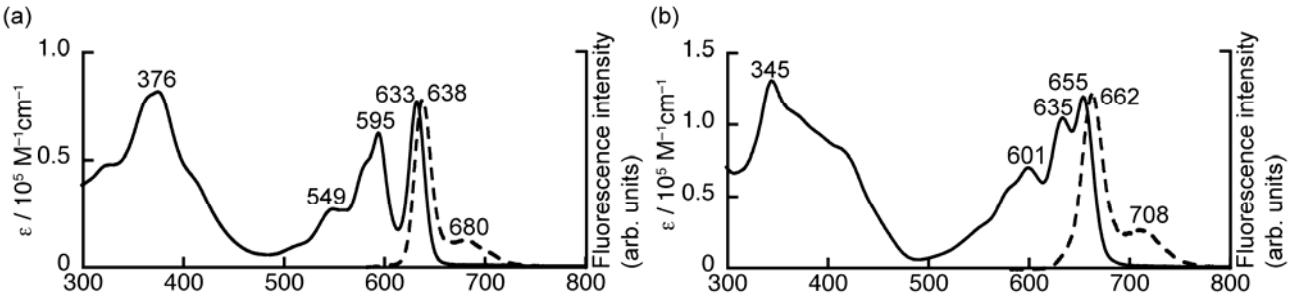

Figure S3. Absorption (solid line) and fluorescence (dashed line) spectra of **3a** (left) and **3b** (right) in $CHCl_3$.

v. DFT and TDDFT calculations of triazaporphyrins

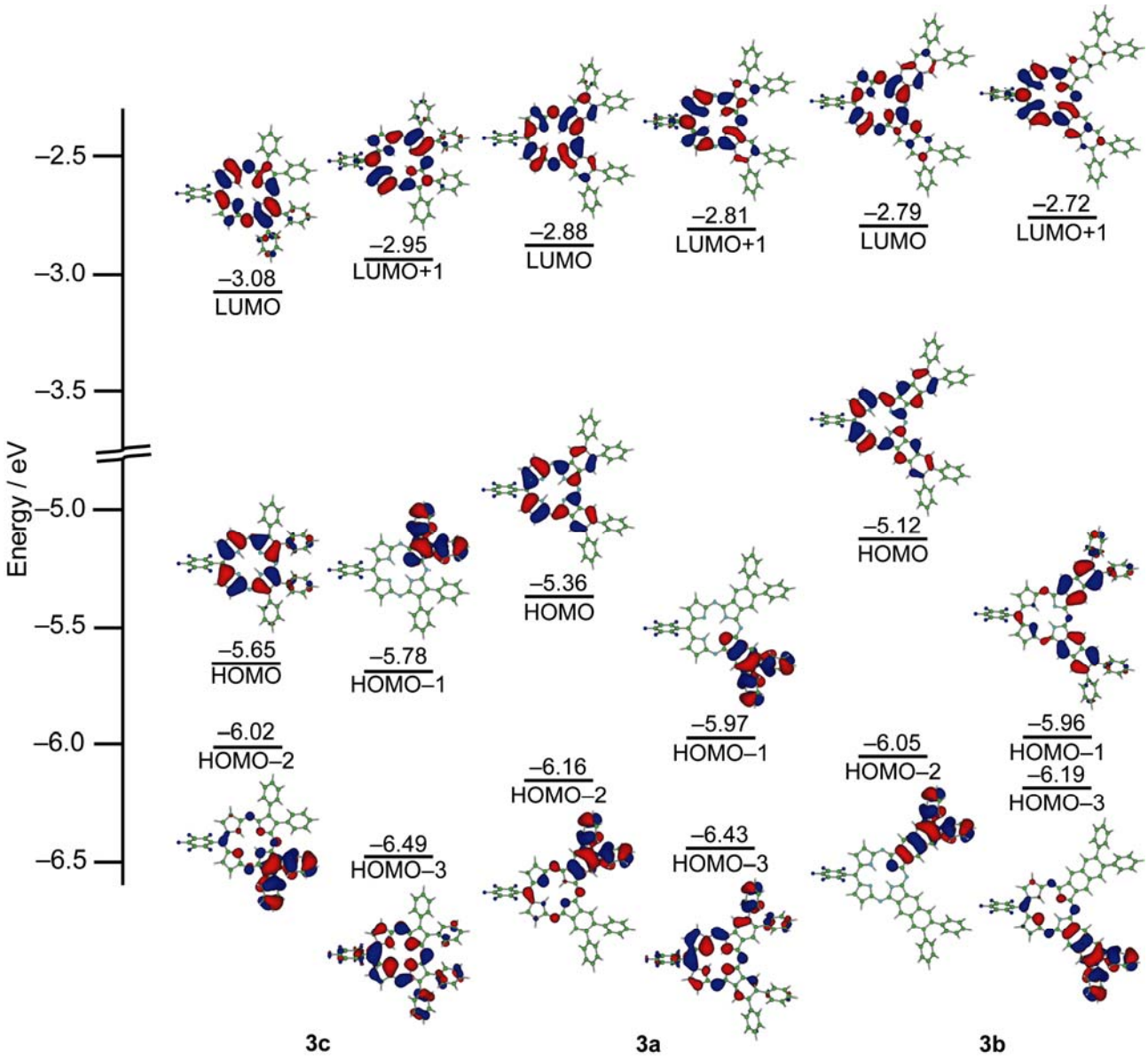

Figure S4. Partial MO diagram of **3a** (middle), **3b** (right), and **3c** (left). Peripheral *p-tert*-butylphenyl substituents ***are included*** in these calculations.

Table S1. Selected transition energies and wave functions of **3a**, **3b**, and **3c** in the Q band region calculated by the TDDFT (B3LYP/6-31G(d)) method. Peripheral *p-tert*-butylphenyl substituents ***are included*** in these calculations.

compd	energy [nm]	*f* [a]	wave function[b]
3a	556	0.27	+ 0.483 | L ← H> + 0.422 | L+1 ← H> + 0.138 | L ← H–3> – 0.144 | L+1 ← H–3> – 0.137 | L ← H–2> + 0.136 | L+1 ← H–2> + …
	539	0.32	+ 0.487 | L+1 ← H> – 0.444 | L ← H> + 0.124 | L ← H–3> + 0.101 | L+1 ← H–3> – 0.134 | L ← H–2> – 0.111 | L+1 ← H–2> + …
3b	583	0.37	+ 0.575 | L+1 ← H> – 0.341 | L ← H> – 0.141 | L ← H–5> – 0.115 | L ← H–3> + …
	579	0.47	+ 0.590 | L ← H> + 0.343 | L+1 ← H> + …
3c	563	0.038	+ 0.604 | L ← H–1> + 0.237 | L ← H> – 0.230 | L+1 ← H–1> + 0.100 | L+1 ← H–2> + …
	553	0.080	+ 0.473 | L ← H> + 0.264 | L+1 ← H> – 0.251 | L ← H–1> + 0.238 | L+1 ← H–2> + 0.186 | L+1 ← H–3> – 0.180 | L ← H–2> – 0.107 | L ← H–3> + …
	536	0.0056	+ 0.657 | L+1 ← H–1> + 0.240 | L ← H–1> + …
	526	0.071	+ 0.477 | L+1 ← H> – 0.365 | L ← H–2> – 0.267 | L ← H> – 0.159 | L+1 ← H–2> – 0.143 | L ← H–3> + 0.103 | L ← H–1> + …
	484	0.21	+ 0.543 | L ← H–2> + 0.298 | L+1 ← H> – 0.316 | L ← H–3> + …
	457	0.24	+ 0.619 | L+1 ← H–2> – 0.225 | L+1 ← H–3> – 0.221 | L ← H> + …

[a] Oscillator strength. [b] Wave functions based on the eigenvectors predicted by TDDFT. H and L represent the HOMO and LUMO, respectively.

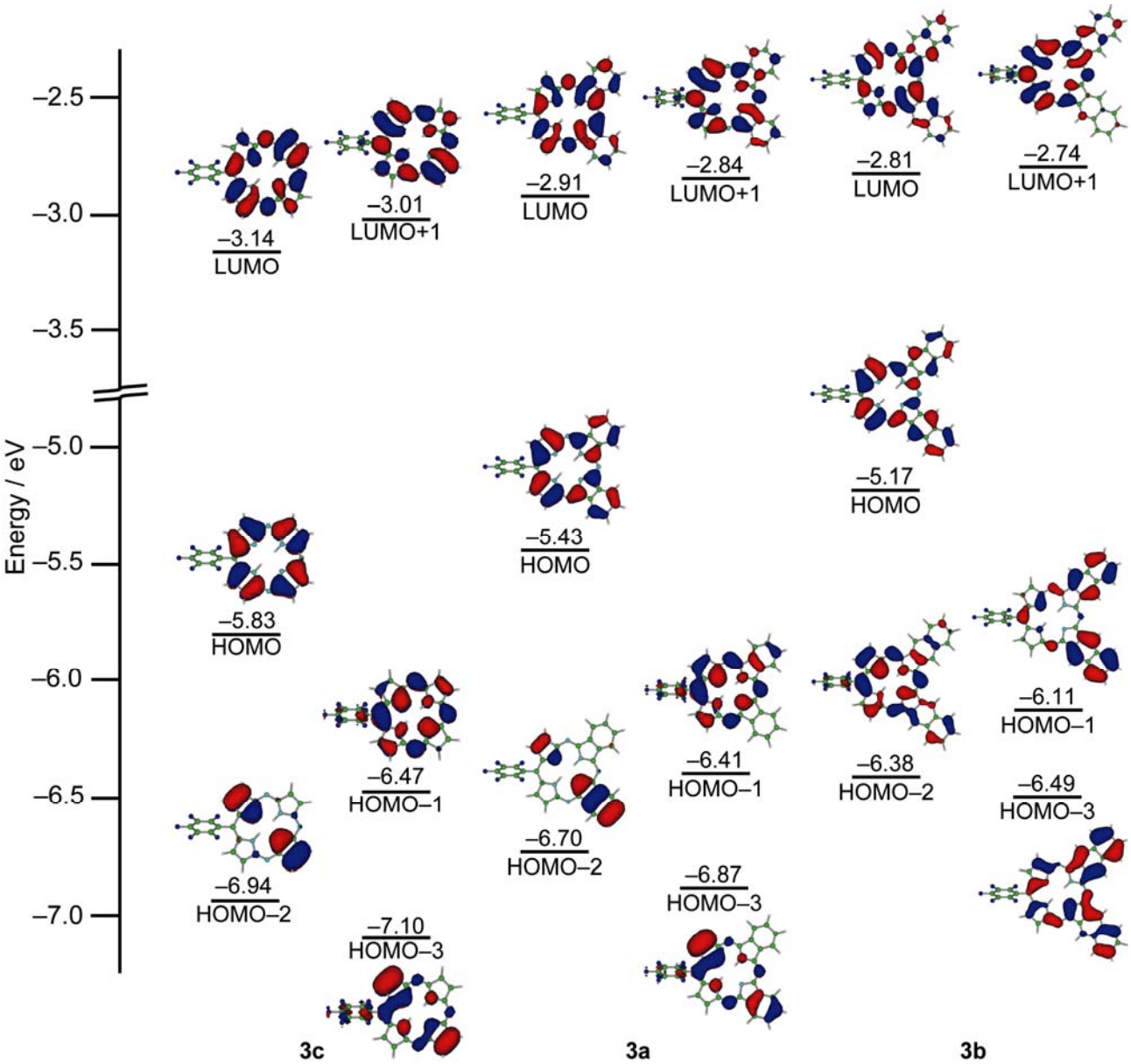

Figure S5. Partial MO diagram of **3a** (middle), **3b** (right), and **3c** (left). Peripheral *p*-*tert*-butylphenyl substituents ***are not included*** in these calculations.

Table S2. Selected transition energies and wave functions of **3a**, **3b**, and **3c** in the Q band region calculated by the TDDFT (B3LYP/6-31G(d)) method. Peripheral *p-tert*-butylphenyl substituents ***are not included*** in these calculations.

compd	energy [nm]	f [a]	wave function[b]
3a	544	0.19	+ 0.489 | L←H> + 0.404 | L+1←H> + 0.204 | L←H–1> – 0.221 | L+1←H–1> +…
	525	0.24	+ 0.494 | L+1←H> – 0.428 | L←H> + 0.200 | L←H–1> + 0.153 | L+1←H–1> +…
3b	574	0.29	+ 0.548 | L+1←H> – 0.376 | L←H> – 0.179 | L←H–2> +…
	568	0.36	+ 0.566 | L←H> + 0.377 | L+1←H> + 0.118 | L+1←H–2> +…
3c	528	0.075	+ 0.523 | L←H> + 0.362 | L+1←H–1> + 0.235 | L+1←H> – 0.195 | L←H–1> +…
	497	0.067	+ 0.524 | L+1←H> – 0.354 | L←H–1> – 0.264 | L←H> – 0.150 | L+1←H–1> +…

[a] Oscillator strength. [b] Wave functions based on the eigenvectors predicted by TDDFT. H and L represent the HOMO and LUMO, respectively.

vi. References

1. G. M. Sheldrick, SHELXL-97, Program for the Solution and Refinement of Crystal Structures, University of Göttingen, Göttingen, Germany, 1997.
2. M. C. Burla, R. Caliandro, M. Camalli, B. Carrozzini, G. L. Cascarano, L. D. Caro, C. Giacovazzo, G. Polidori, and R. Spagna, *J. Appl. Crystallogr.*, 2005, **38**, 381.
3. Yadokari-XG, Software for Crystal Structure Analyses, K. Wakita, (2001); Release of Software (Yadokari-XG 2009) for Crystal Structure Analyses, C. Kabuto, S. Akine, T. Nemoto, and E. Kwon, *J. Cryst. Soc. Jpn.*, 2009, **51**, 218.
4. Gaussian 09, Revision A.02, M. J. Frisch, G. W. Trucks, H. B. Schlegel, G. E. Scuseria, M. A. Robb, J. R. Cheeseman, G. Scalmani, V. Barone, B. Mennucci, G. A. Petersson, H. Nakatsuji, M. Caricato, X. Li, H. P. Hratchian, A. F. Izmaylov, J. Bloino, G. Zheng, J. L. Sonnenberg, M. Hada, M. Ehara, K. Toyota, R. Fukuda, J. Hasegawa, M. Ishida, T. Nakajima, Y. Honda, O. Kitao, H. Nakai, T. Vreven, J. A. Montgomery, Jr., J. E. Peralta, F. Ogliaro, M. Bearpark, J. J. Heyd, E. Brothers, K. N. Kudin, V. N. Staroverov, R. Kobayashi, J. Normand, K. Raghavachari, A. Rendell, J. C. Burant, S. S. Iyengar, J. Tomasi, M. Cossi, N. Rega, J. M. Millam, M. Klene, J. E. Knox, J. B. Cross, V. Bakken, C. Adamo, J. Jaramillo, R. Gomperts, R. E. Stratmann, O. Yazyev, A. J. Austin, R. Cammi, C. Pomelli, J. W. Ochterski, R. L. Martin, K. Morokuma, V. G. Zakrzewski, G. A. Voth, P. Salvador, J. J. Dannenberg, S. Dapprich, A. D. Daniels, O. Farkas, J. B. Foresman, J. V. Ortiz, J. Cioslowski, and D. J. Fox, Gaussian, Inc., Wallingford CT, 2009.
5. M. S. Rodríguez-Morgade, M. Planells, T. Torres, P. Ballester, and E. Palomares, *J. Mater. Chem.*, 2008, **18**, 176.